Solid-state chemistry and non-linear properties of tetragonal tungsten bronzes materials

Annie Simon, Jean Ravez

Solid-state chemistry and non-linear properties of tetragonal tungsten bronzes materials

Annie Simon *, Jean Ravez

ICMCB–CNRS, université Bordeaux-1, 87, avenue Albert-Schweitzer, 33608 Pessac cedex, France

Abstract

Non-linear properties of tetragonal tungsten bronze materials are related to solid-state chemistry. This family is very prolific, with its five different cationic or anionic crystallographic sites. The physical characteristics are correlated to composition and chemical bonding. Some effective or potential applications are described. ***To cite this article: A. Simon, J. Ravez, C. R. Chimie 9 (2006)***.

Résumé

Les propriétés non linéaires des matériaux de type bronzes quadratiques de tungstène sont décrites et discutées sur le plan de la chimie du solide. Cette famille est très prolifique, en raison, en particulier de ses cinq sites cristallographiques cationiques ou anioniques. Les caractéristiques physiques sont corrélées à la composition et à des considérations de liaison chimique. Enfin, quelques applications réelles ou potentielles sont décrites. ***Pour citer cet article : A. Simon, J. Ravez, C. R. Chimie 9 (2006)***.

Keywords: Tetragonal tungsten bronzes

Mots clés : Bronzes de tungstène quadratiques

1. Introduction

Tetragonal tungsten bronze (TTB) structure was determined in 1949 by Magneli [1] on $K_{0.57}WO_3$ ($K_{2.85}W_5O_{15}$). In 1953, ferroelectric properties were evidenced on $PbNb_2O_6$ ($Pb_{2.5}Nb_5O_{15}$) [2]. In 1967, non-linear optics properties were studied on TTB crystals in IBM and Bell Telephone Laboratories [3]. From 1970, dielectric studies were carried out simultaneously in the USA, the USSR, Japan, Great Britain and France.

The present work refers to solid-state chemistry and non-linear properties (ferroelectricity, ferroelasticity, ferromagnetism, non-linear optics…) in TTB type materials. These properties are so called due to the main physical characteristics that display a non-linear variation (hysteresis loop) with external stress: polarization–electric field, strain–mechanical stress, magnetization–magnetic field… Relaxors will be also described. Materials involved are either ceramics or single crystals. Works on thin films are topical subject up to date.

2. Crystal chemistry

2.1. Crystal structure

Fig. 1 shows a schematic representation of the TTB structure projection along the [001] direction. For a general $A_2BC_2M_5X_{15}$ (X = O, F) formulation, large ca-

* Corresponding author.
E-mail address: simon@icmcb-bordeaux.cnrs.fr (A. Simon).

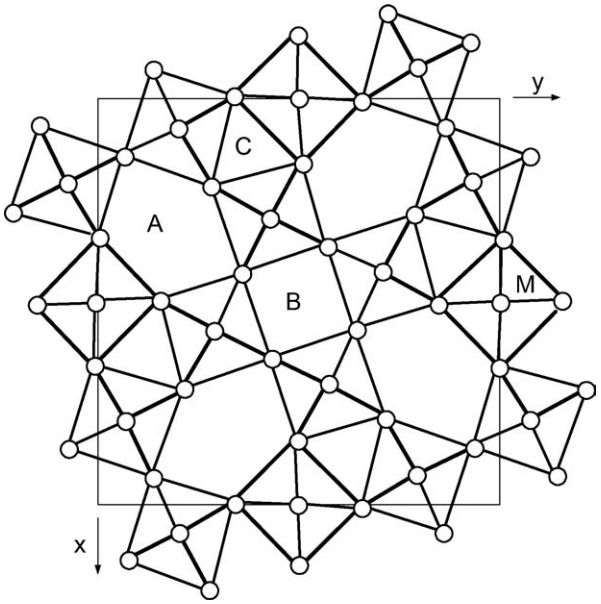

Fig. 1. Schematic projection of the TTB crystalline network along the fourfold *c* axis (A, B and C correspond to cationic sites with 15, 12 and 9 coordination numbers, respectively, in unit cell $A_2BC_2M_5X_{15}$).

tions occupy the pentagonal 15 C.N. (A) and square 12 C.N. (B) sites, small cations are in the triangular 9 C.N. (C) sites, and small and highly charged cations are in the octahedral M sites.

2.2. Ion localization

Table 1 gives the localization of various ions (or chemical entities) in the different crystallographic sites. The chemical stability is the highest when:

- big cations (e.g., Ba^{2+} or Pb^{2+}) occupy an A site;
- small and low-charged cations (e.g. a Li^{+}) are in C site;
- small and highly charged cations (e.g., Nb^{5+}, Ta^{5+}) are in a M site;
- for high-oxygen-rate compositions (e.g., O_{15});
- for high-fluorine-rate compositions (e.g., F_{15}).

The various types of stoichiometry depend on the existence of vacancies (□) in either one or another site:

- all sites full: $A_2BC_2M_5X_{15}$ (e.g., $K_3Li_2Nb_5O_{15}$);
- half C sites empty: $A_2BC\square M_5X_{15}$ (e.g., $K_3NiNb_5O_{15}$);
- C sites empty: $A_2B\square_2M_5X_{15}$ (e.g., $Ba_2NaNb_5O_{15}$);
- B and C sites empty: $A_2\square\square_2M_5X_{15}$ (e.g., $BaBiNb_5O_{15}$).

Table 1
Localization of various ions or chemical groupements in the different crystallographic sites

A [15 C.N.]	K^{+}, Rb^{+}, Cs^{+}, Tl^{+} Ca^{2+}, Sr^{2+}, Ba^{2+}, Pb^{2+}, (M–O–M) chains (M = Nb, Ta, Mo, W)
B [12 C.N.]	Na^{+}, K^{+}, Ag^{+} Ca^{2+}, Sr^{2+}, Ba^{2+}, Cd^{2+}, Eu^{2+}, Pb^{2+} Ln^{3+},…, Bi^{3+} Ce^{4+}, Th^{4+}, U^{4+}…
C [9 C.N.]	Li^{+}, Na^{+} Mg^{2+}, Ni^{2+}, Cu^{2+}… Li^{+}
M [6 C.N.]	Mg^{2+}, V^{2+}, Fe^{2+}, Co^{2+}, Ni^{2+}, Cu^{2+}, Zn^{2+} V^{3+}, Mn^{3+}, Fe^{3+} Ti^{4+}, Zr^{4+}, Sn^{4+}, Nb^{4+} V^{5+}, Nb^{5+}, Ta^{5+}, W^{5+} Mo^{6+}, W^{6+}
X	F^{-}, O^{2-}

Several solid solutions can be obtained between each kind of non-stoichiometric compositions (e.g. $(Ba_{1.5}Sr_{0.5})(Sr_{0.5}\square_{0.5})\square_2Nb_5O_{15}$).

2.3. Phase transitions

In TTB crystals, there is a permanent anisotropy, even in centrosymmetric phases; it is not thus possible to reach the cubic symmetry. The prototype high temperature variety is tetragonal (4/*mmm*). The following Table 2 gives the various phase transition sequences with the corresponding properties as described in sections 3 and 5 [4]:

- no transition: it is the case of oxyfluorides with a relatively high fluorine substitution rate; very low degree of covalence in octahedral bonds prevent the formation of non-centro-symmetric phase;
- one transition: when the temperature decreases, a ferroelectric phase appears in either the tetragonal system (4*mm*) or the orthorhombic one (*mm*2) giving rise here to ferroelastic properties. Polar axis is along [001] for spherical cations (e.g., alkaline and alkaline earth cations); it is oriented along [010] when cations with $6s^2$ lone pair, easily polarizable, are introduced (Tl^{+}, Pb^{2+}, Bi^{3+});
- two transitions: compounds with tantalum belong to this family (Table 2);
- three transitions were announced for $Ba_2NaNb_5O_{15}$: a ferroelastic phase is included between two other more symmetric phases with the same point space group [5]. Such a transition sequence is in fact more

Table 2
Transition sequences of phases with tetragonal tungsten bronze structure

N [a]	Compositions	Transitions sequences						
0	$K_3Nb_5O_{13}F_2$	4/*mmm* paraelectric paraelastic						
1	$K_3Li_2Nb_5O_{15}$	4*mm* ferroelectric [001] paraelastic	⇒	4/*mmm* paraelectric paraelastic				
	$Sr_2K_{0.5}Li_{0.5}$ Nb_5O_{15}	*mm*2 ferroelectric [001] ferroelastic	⇒	4/*mmm* paraelectric paraelastic				
	$Pb_2KNb_5O_{15}$	*mm*2 ferroelectric [010] ferroelastic	⇒	4/*mmm* paraelectric paraelastic				
2	$Sr_2KTa_5O_{15}$	*mm*2 ferroelectric [001] ferroelastic	⇒	*mmm* paraelectric ferroelastic	⇒	4/*mmm* paraelectric paraelastic		
	$Pb_{2.07}K_{0.56}Nb_{0.91}$ $Ta_{4.15}O_{15}$	*mm*2 ferroelectric [010] ferroelastic	⇒	*mmm* paraelectric ferroelastic	⇒	4/*mmm* paraelectric paraelastic		
3	$Ba_2NaNb_5O_{15}$	4*mm* ferroelec. [001] paraelastic	⇒	*mm*2 ferroelec. [001] ferroelastic	⇒	4 *mm* ferroelec. [001] paraelastic	⇒	4/*mm* paraelectric paraelastic
	$Ba_{2.14}Li_{0.71}Nb_{2.5}$ $Ta_{2.5}O_{15}$	222 antiferroelec. ferroelastic	⇒	*mm*2 ferroelec. [001] ferroelastic	⇒	$\bar{4}2m$ paraelec. paraelastic	⇒	4/*mmm* paraelectric paraelastic

[a] Transition number.

complicated with appearance of incommensurate phases. From room temperature to 523 K, the first incommensurate phase is nearly commensurate. On the contrary, from 523 to 561 K, the corresponding phase is clearly incommensurate. These anomalous effects were attributed to the influence of defects having their origin in either an off-stoichiometry or off-equilibrium distribution of the cations in the structure [6].

3. Ferroelectricity

3.1. Generalities

Dielectric and pyroelectric studies have shown several TTB non-centrosymmetric phases to be ferroelectric. The values of T_c of the various samples are between 7 K ($K_3Li_2Ta_5O_{15}$) and 899 K ($Ba_{2.02}Li_{0.96}Nb_5O_{15}$). Fig. 2 gives, as an example, the temperature dependence of the permittivity ε'_r for a ceramic with $Pb_2KNb_5O_{15}$ composition.

3.2. Origin of the ferroelectricity

Ferroelectrics may be divided into two basic types ('displacive' and 'order–disorder'):

- *Displacive ferroelectrics*: in the paraelectric phase, the small charged cation (e.g., Nb^{5+} in $Ba_2KNb_5O_{15}$) is situated at the barycentre of the oxygen octahedron. The polar variety is characterized by correlated shifts of the Nb^{5+} ions away from the centre of gravity of the octahedra.
- *Order–disorder ferroelectrics*: while the ions in the paraelectric phase are located randomly in equiva-

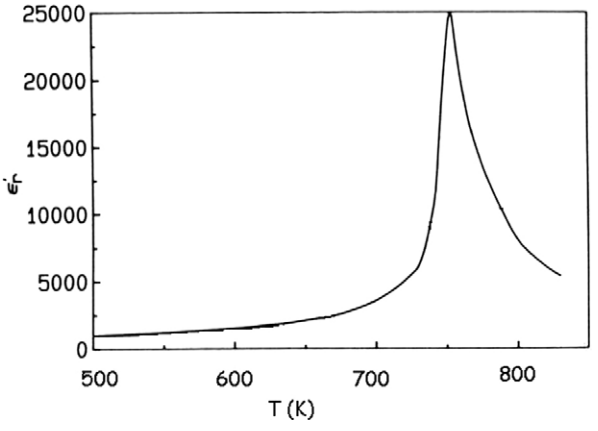

Fig. 2. Temperature dependence of the permittivity ε'_r for a ferroelectric ceramic: $Pb_2KNb_5O_{15}$.

lent sites within the polar phase, they are preferentially positioned in some of these sites, thus giving rise to local polarization and thus ferroelectricity. The fluoride $K_3Fe_5F_{15}$ of mixed valency is an interesting example: in this case, it is the Fe^{2+} and Fe^{3+} ions that are arranged in non-equivalent octahedral sites [$K_3Fe^{2+}(Fe^{2+}{}_2Fe^{3+}{}_2)F_{15}$] by shifts along the polar axis.

3.3. Relation between composition, Curie temperature and chemical bonding

For a given structural type, the value of T_c depends on the composition. The variations of T_c may be correlated with factors of chemical bonding such as size, coordination or electronic configuration of cations, bond covalency, order–disorder, etc. [7,8].

3.3.1. Size of cations in the 6-coordination site

The value of T_c decreases as the size of the M^{n+} ion increases. For the substitution Zr–Ti, for example, it is the largest size of Zr^{4+} that limits its shift Δz, thereby leading to a decrease in T_c [9] (e.g., $T_c = 518$ K ($Ba_3TiNb_4O_{15}$); $T_c = 310$ K ($Ba_3ZrNb_5O_{15}$)).

3.3.2. Size of cations outside of octahedra

A decrease in the size of ion A^{n+} leads to a decrease in T_c as long as its environment remains spherical and its coordination is not modified. Here are some characteristic examples ($r_{Ba}{}^{2+} > r_{Sr}{}^{2+}$) [9]:

Compounds	T_c (K)
$Ba_2NaNb_5O_{15}$	853
$Sr_2NaNb_5O_{15}$	539
$Ba_2KNb_5O_{15}$	665
$Sr_2KNb_5O_{15}$	429
$Ba_3(TiNb_4)O_{15}$	518
$Sr_3(TiNb_4)O_{15}$	403

3.3.3. Bond covalency

The following three examples show this influence in displacive type ferroelectrics:

- the substitution Ta–Nb in the octahedral site leads to a large decrease in T_c. The cations Nb^{5+} and Ta^{5+} have similar charges, configurations and size [9]. Therefore, this is the effect of the covalence of the M–O bonds (M = Nb, Ta). In relatively covalent compositions such as the niobates, the increase in covalence (substitution Ta–Nb) arising from the more diffuse character of the wave function of Ta, i.e. a larger M–O overlap for M = Ta, leads to a drop in T_c owing to the hardening or rigidification of the crystalline network, which thus cancels the ferroelectric distortion [10];
- the substitution F–O rapidly makes the network more ionic, since it leads to a decreased octahedral distortion. In most iono-covalent networks, this induces a spectacular drop in T_c (Table 3) [11];
- an apparently unexpected case combines the two precedent phenomena. It concerns the F–O substitution in the very covalent network of some tantalates. For example, although in the niobate $K_3Li_2Nb_5O_{15}$ ($T_c = 703$ K), the F–O substitution leads to a very sharp drop in T_c, in the tantalate $K_3Li_2Ta_5O_{15}$ ($T_c = 7$ K), T_c increases ($T_c = 80$ K) for $K_3Li_{1.5}Ta_5O_{14.5}F_{0.5}$. In this case, it is the decrease in covalence due to the F–O substitution, which leads to a lesser hardening of the network, and thus to a slight increase in both the ferroelectric distortion and T_c [12].

3.3.4. Fluorides

As seen in section 3.2., such ferroelectrics are of order–disorder type. The values of T_c are here relatively high ($T_c = 495$ K for $K_3Fe_5F_{15}$) [13].

3.3.5. Particular configurations of cations

The lone pair occurs for the Tl^+, Pb^{2+} and Bi^{3+} cations. The increase in T_c is due to this lone pair, which leads to a non-spherical cation. An example concerns $K_2BiNb_5O_{15}$ ($T_c = 633$ K), which has a higher T_c value than those of $K_2LaNb_5O_{15}$ ($T_c = 180$ K) or $K_2NdNb_5O_{15}$ ($T_c = 442$ K) [9].

3.3.6. Cationic order

An order within the crystalline network favours a cooperative effect, which in turn highly distorts the structure and induces an increase in T_c. This effect may be demonstrated with the four following compounds: $Sr_2KNb_5O_{15}$ ($T_c = 429$ K), $Sr_2NaNb_5O_{15}$ ($T_c = 539$ K), $Ba_2KNb_5O_{15}$ ($T_c = 665$ K), $Ba_2NaNb_5O_{15}$ ($T_c = 853$ K). This distortion is not really enhanced by the disordered distribution of the alkaline earth cations and potassium in the sites of coordination 15 and 12, owing to their comparable size [9]. The polar phases remain tetragonal like the paraelectric phase. On the other hand, the smaller Na^+ ion is preferentially positioned in the site

Table 3
Variation of T_c with the F–O substitution rate

Compositions	ΔT_c (K) [a]
$(Sr_{2-x}K_{1+x})Nb_5O_{15-x}F_x$	140
$(Ba_{2-x}Na_{1+x})Nb_5O_{15-x}F_x$	660
$Sr_2K(Nb_{5-x}Ti_x)O_{15-x}F_x$	210
$Ba_2Na(Nb_{5-x}Ti_x)O_{15-x}F_x$	115

[a] Normalized variation of T_c for a ratio F/(F+O) varying from 0 to 10^{-2}.

of coordination 12; the alkaline earth cations, which are twice as numerous, are situated naturally in the sites of coordination 15, themselves also twice as numerous.

3.4. Prediction of ferroelectricity

The transition from paraelectric to ferroelectric phase can occur through atomic shifts associated with distortion and/or rotation of octahedra. In both cases, when there is a transition from the non-polar to the polar form, low-amplitude atomic shifts Δz occur (< 1 Å) in the direction of the polar axis, thus giving a resultant polarization along the same axis. An empirical relationship between T_c and Δz has been demonstrated: $T_c = 2 \times 10^4 (\Delta z)^2$ (Å^2) [14].

Examination of the atomic positions of a polar crystalline network (having no centre of symmetry but a polar axis) makes it possible not only to predict the ferroelectric properties but also the value corresponding of T_c. Such relation was applied for various TTB crystals derived from $(Ba,Sr)_{2.5}Nb_5O_{15}$, $K_3Li_2Nb_5O_{15}$…

4. Relaxors

4.1. Introduction

According to their particular dielectric behaviour, materials may be divided into two different classes, depending on whether they are classical ferroelectric or relaxor:

- a maximum of ε'_r and a value of the Curie temperature T_c, no frequency-dependent for ferroelectrics;
- a maximum of ε'_r at a temperature called T_m, the two corresponding values varying with frequency for relaxors [15].

Concerning the relaxors, at least two different cations have to be localised in the same crystallographic site. Although relaxors have no macroscopic polarization (thus no P–E hysteresis loop), they are of great interest for dielectrics in capacitors and actuators [16]. The relaxor materials usually used are perovskite lead-based ceramics, for example $PbMg_{1/3}Nb_{2/3}O_3$ (PMN) and derived compounds. To date, various physical models have been described to explain the properties of relaxors [17]: compositional fluctuations and diffuse phase transition [18,19], the superparaelectric model [20], the nanostructure-octahedral model [21–24], the dipole-glass or the more recent derived model [25], the random-field model [26], the domain-wall model [27] and the random-layer model [28].

4.2. Lead-based TTB relaxors

Contrary to the perovskite class, the TTB Pb-based relaxors are not very numerous and have not been widely studied. However, some recent studies have been dedicated to this material class [17,29]. As an example, Fig. 3 shows the temperature dependence of ε'_r at various frequencies. At least one cation ferroelectrically active in the octahedral site must be present. The

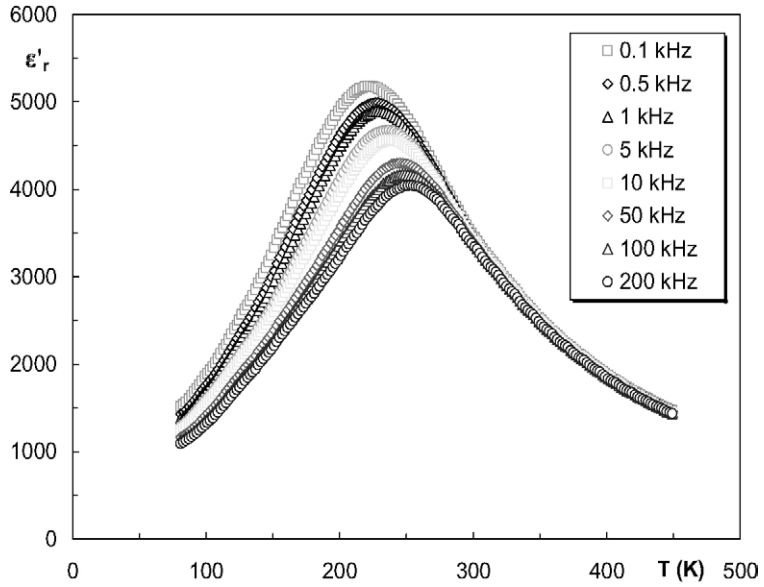

Fig. 3. Temperature and frequency dependences of the permittivity ε'_r for a relaxor ceramic $Sr_2K(Nb_{0.775}Ta_{0.225})O_{15}$.

relaxor effect is simultaneously due to a disorder of the lead position and to a disorder of the cationic distribution in the A and B sites. The substitutions in the M site induce a relaxor state if the long-range order is not induced by a local dipolar order (e.g., tantalates).

4.3. Lead-free TTB relaxors

Such materials are of great interest as environment-friendly applications. The first compositions announced as relaxors concerned the $Ba_{2.5(1-x)}Sr_{2.5x}Nb_5O_{15}$ solid solution [30–32]. Very recently, relaxor behaviour was demonstrated in other compositions: e.g. $BaLaNb_5O_{15}$, $BaBiNb_5O_{15}$, $SrK_2Nb_5O_{14}F$, $BaNa_2Nb_5O_{14}F$… [33]. Some solid solutions situated between classical ferroelectric and relaxor have also been studied. Such is the case with $A_2B(Nb_{1-x}Ta_x)_5O_{15}$: the replacement of very ferroelectrically active Nb^{5+} by the less active Ta^{5+} transforms the macroscopic polarization into a local one for the highest values of x. This is also the case with the $Ba_2NaNb_5O_{15}$–$BaNa_2Nb_5O_{14}F$ system; for compositions close to the oxide, the behaviour is ferroelectric, while it becomes relaxor when the fluorine rate and thus the sodium rate is sufficiently high (Fig. 4) [34]. The frequency dependence of the permittivities of a ceramic with a composition $BaNa_2Nb_5O_{14}F$ clearly displays a frequency relaxation at 77 K, while it disappears at 300 K, i.e. for $T > T_m$ (T_m = 140 K at 10^3Hz) (Fig. 5). The crystal structure determination of this compound is in good agreement with the dielectric properties: the A-site is statistically occupied by equal quantities of Ba^{2+} and Na^+, thereby giving a cationic disorder in this A-site, while the B-site is filled by Na^+ cations [35].

Of all the lead-free compounds studied, it is with Bi^{3+}, another 6 $(sp)^2$ lone pair cation, that the highest value of T_m was obtained: T_m ($BaBiNb_5O_{15}$ = 319 K at 10^3 Hz). Such a result is in good agreement with that obtained for lead-free compositions derived from $BaTiO_3$ [36].

5. Ferroelasticity

The paraelectric-ferroelectric transition may be effected either without change of crystalline system (4/*mmm* → 4*mm*), or with the appearance of an orthorhombic symmetry due to slight distortions (4/*mmm* → *mm*2). In the last case, the ferroelectric phase has also ferroelastic properties.

When inserted cations in sites of 15- and 12-fold coordinations are alkaline or alkaline-earth ions (e.g., $Ba_2NaNb_5O_{15}$), the polar axis is along the [001] direction [37]. The switching of the polarization direction does not entail the passage from one ferroelastic state to another and inversely, the elastic transformation from state one to state two by the application of a mechanical stress does not change the sense of the polarization. Thus ferroelastic–ferroelectric properties are decoupled (Fig. 6).

On the contrary, if the inserted cation possesses a $6s^2$ lone pair (Tl^+, Pb^{2+}, Bi^{3+}), the polar axis is along [010]

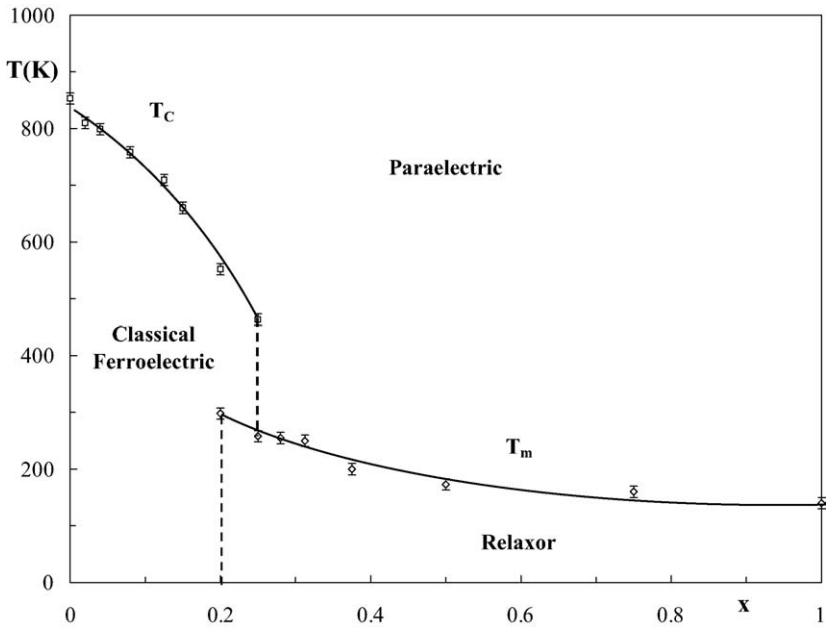

Fig. 4. Variation of transitions temperatures with x for ceramics with composition $Ba_{2-x}Na_{1+x}Nb_5O_{15-x}F_x$.

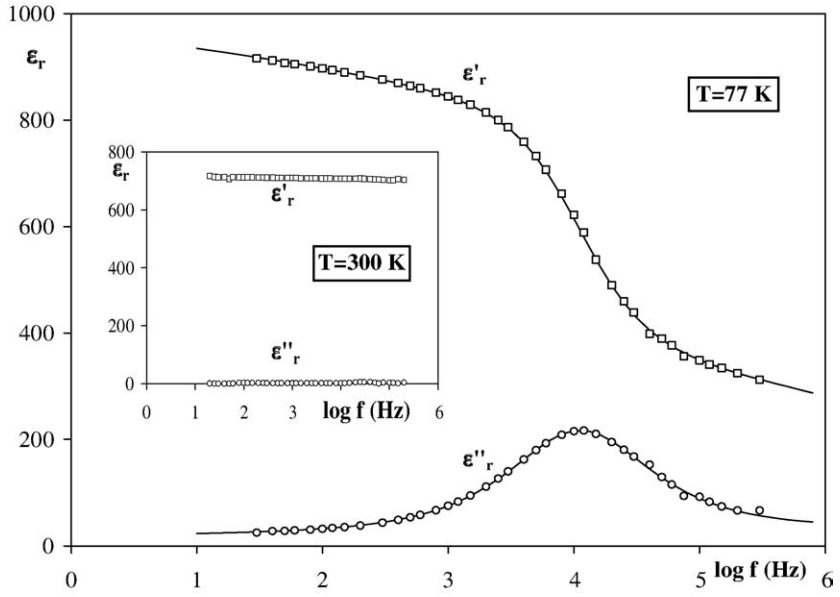

Fig. 5. Frequencies dependences of the permittivities ε'_r and ε''_r for a ceramic with composition $BaNa_2Nb_5O_{14}F$. The dashed line shows the fit of data according to the Cole–Cole model.

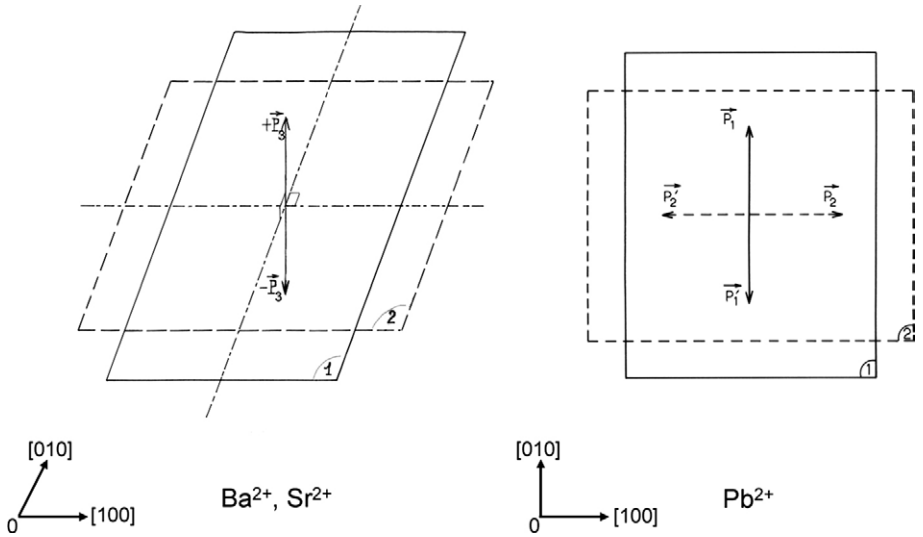

Fig. 6. Nature of spontaneous strains and polarizations in crystalline phases with TTB structure.

and simultaneously the *b* parameter is higher than the *a* one [38,39]. We may foresee that the application of an electric field along O*x* would produce a rotation of polarization by 90° and consequently the passage from an elastic state to another. In the same way, the change from state one to state two would lead to the rotation of the polar axis by 90°. The ferroelastic–ferroelectric properties would then be partially coupled. Such a prediction was proved on a lead potassium niobotantalate crystal [40].

6. Non-linear optics

The second harmonic generation efficiency E_{SHG} is the rate of conversion of a fundamental wave into a second harmonic wave (100 $I_{2\omega}/I_{\omega}$). It is usually expressed as a relative value compared to that of a reference compound, e.g., KH_2PO_4 (KDP), quartz α.

Ferroelectric materials (non-centrosymmetric and polar) have very high non-linear susceptibilities. The higher the spontaneous polarization P_s, T_c and Δz (see

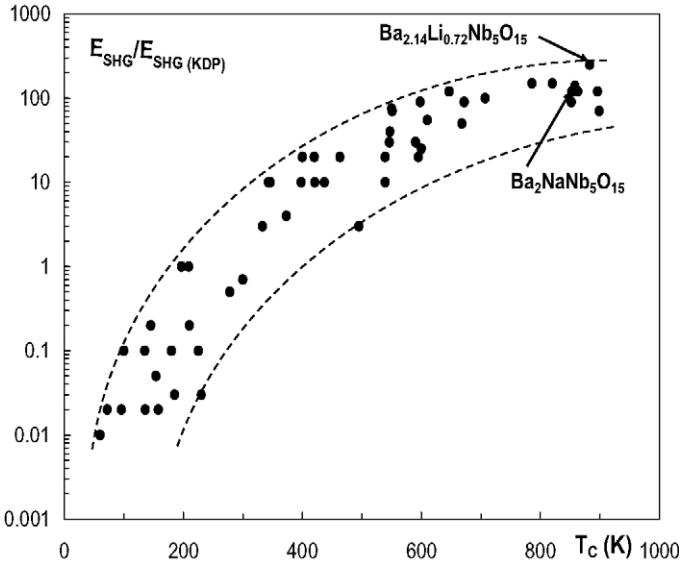

Fig. 7. Variation of SHG efficiency of TTB-type materials in relation to KDP as T_c changes.

Section 3.4), the greater the tensor coefficients and the harmonic yield [41]. As an example, Fig. 7 shows the variation in $E_{SHG}/E_{SHG}(KDP)$ versus T_c [42]. $Ba_2NaNb_5O_{15}$, $Ba_{2.14}Li_{0.72}Nb_5O_{15}$) are among the most efficient compositions in order to be used in application field.

However, other factors are to be considered to obtain a maximal efficiency, i.e. crystal size and optical quality phase matching.

7. Ferromagnetism

Such a non-linear behaviour occurs in fluorides. As examples:

- in the $(1–x)$ Mn^{2+}–x Co^{2+} substitution from $K_{2.5}(Mn_{2.5}Fe_{2.5})F_{15}$, there is coexistence of antiferromagnetic and ferromagnetic short-range correlations above T_N in the samples with a Co^{2+} concentration in the range $0.6 < x < 1$. Such a behaviour was also obtained for compositions containing Mn^{2+} and Cr^{3+} cations [43,44];
- in $K_{5x}(M_x{}^{2+}M_{1-x}{}^{3+})_5F_{15}$ with $0.4 < x < 0.6$, M^{2+} = Mn, Ni and M^{3+} = V, Cr, magnetic ordering occurs in two steps. Linear trimers $(M^{2+})_3$ and $(M^{3+})_3$ form exist, giving rise to a quasi-paramagnetic region, followed at lower temperature by long-range magnetic ordering. The 180° M^{2+}–F^-–M^{3+} magnetic interactions appear to be ferromagnetic [13];
- the composition $K_3Fe_5F_{15}$ is a multiferroic system. Ferroelasticity and ferroelectricity are coupled at temperature lower than $T_c = 490$ K. In addition, a spontaneous ferromagnetic component appears below 120 K, in the magnetically ordered phase [13,45,46].

8. Applications

Up-to-date TTB-type materials are now mainly used as single crystals, e.g.:

- strontium barium niobates as infrared detectors;
- barium sodium niobates as electro-optics modulators, parametric modulators or frequency doublers [47–50].

Elsewhere acoustic applications (e.g., sonars) require a very high k_{33} electromechanical coupling coefficient. Unfortunately, big single crystals, useful for such an application, are often very difficult to elaborate. In this way, the current researches are oriented toward texturised ceramics. Such materials are prepared using small ‘non-cubic’ single crystals, obtained by flux methods and mixed with nanometric powder. Before sintering, it is necessary to line up the small single crystals in the same direction. TTB ferroelectric compositions possess a high value of k_{33}, a tetragonal prototype phase and crystallise as long straight prism with a small square-base morphology. They are thus very promising candidates [51]. In addition, current researches are related to spread the application domain to TTB type thin films.

9. Conclusions

The TTB compositions are oxides, oxyfluorides or fluorides. The great ability of this prolific family to give various crystallographic distortions leads to performing ferroelastic and ferroelectric properties. Their physical characteristics (ferroelectric or ferroelastic Curie temperature T_c, spontaneous strain or polarization) can be related to cationic size and charge, bond covalency and cationic order. An interesting result concerns the oxyfluorides ferroelectric (of displacive type) in which the value of T_c decreases strongly with the fluorine substitution rate; however the pure fluorides (of ferroelectric order–disorder type) show unexpected high values of T_c. The TTB materials are able to lead to a relaxor behaviour due to cationic disorder in one or another crystallographic site. The compositions with a high ferroelectric Curie temperature show a high second harmonic generation efficiency (non-linear optics). A ferromagnetic component was observed in fluorides containing transition element cations; the values of T_N are nevertheless low. Some considerations of present or future applications were discussed. The non-cubic state of the prototypic phase is interesting for texturised ceramics in the way of acoustic applications. Also, lead-free compositions are of interest as environment-friendly applications.

References

[1] A. Magneli, Ark. Kemi 24 (1949) 213.
[2] M.H. Francombe, B. Lewis, Acta Crystallogr. 11 (1958) 696.
[3] J.E. Geusic, H.J. Levinstein, J.J. Rubin, S. Singh, L.G. Van Uitert, Appl. Phys. Lett. 11 (1967) 269.
[4] J. Ravez, P. Hagenmuller, Mater Res. Bull. 12 (1977) 769.
[5] J. Schneck, J. Primot, R. Von Der Mühll, J. Ravez, Solid-State Commun. 21 (1977) 57.
[6] J. Schneck, J.C. Toledano, C. Joffrin, J. Aubree, B. Joukoff, A. Gabelotaud, Phys. Rev. B 25 (3) (1982) 1766.
[7] J. Ravez, A. Perron-Simon, P. Hagenmuller, Ann. Chim. 1 (1976) 251.
[8] J. Ravez, M. Pouchard, P. Hagenmuller, Eur. J. Solid-State Inorg. Chem. 28 (1991) 1107.
[9] R.D. Shannon, Acta Crystallogr. A 32 (1976) 751.
[10] T. Neumann, G. Borstel, C. Scharfschwerdt, M. Neumann, Phys. Rev. B 46 (1992) 10623.
[11] J. Ravez, C. R. Acad. Sci., 2, Ser. IIc, Paris, 1999 (11) 415.
[12] A. Villesuzanne, C. Elissalde, M. Pouchard, J. Ravez, Eur. Phys. J. B 6 (1998) 307.
[13] J. Ravez, S.C. Abrahams, R. De Pape, J. Appl. Phys. 65 (1989) 3987.
[14] S.C. Abrahams, S.K. Kurtz, B. Jamieson, Phys. Rev. 172 (1968) 551.
[15] L.E. Cross, Ferroelectrics 151 (1994) 305.
[16] K. Uchino, Ferroelectrics 151 (1994) 321.
[17] V. Hornebecq, C. Elissalde, F. Weill, A. Villesuzanne, M. Ménétrier, J. Ravez, J. Appl. Crystallogr. 33 (2000) 1037.
[18] G. Smolenski, A. Agranovskaya, Sov. Phys. Solid State 1 (1960) 1429.
[19] B. Rolov, Sov. Phys. Solid State 6 (1965) 1976.
[20] L.E. Cross, Ferroelectrics 76 (1987) 241.
[21] C.A. Randall, A.S. Bhalla, Jpn J. Appl. Phys. 29 (1990) 327.
[22] N.W. Thomas, J. Phys. Chem. Solids 51 (1990) 1419.
[23] H.D. Rosenfeld, E. Egami, Ferroelectrics 158 (1994) 351.
[24] H. Qian, L.A. Bursill, Int. J. Mod. Phys. B 10 (1996) 2027.
[25] D. Viehland, M. Wuttig, L.E. Cross, Ferroelectrics 120 (1991) 71.
[26] V. Westphall, W. Kleeman, M.D. Glinchuk, Phys. Rev. Lett. 68 (1992) 847.
[27] I.W. Chen, Y. Wang, Ferroelectrics 206–207 (1998) 245.
[28] T. Egami, Ferroelectrics 222 (1999) 163.
[29] P. Sciau, G. Galvarin, J. Ravez, Acta Crystallogr. B55 (1999) 459.
[30] P.B. Jamieson, S.C. Abrahams, J.L. Bernstein, J. Chem. Phys. 48 (1968) 5048.
[31] D. Viehland, S. Jang, L.E. Cross, Philos. Mag. B64 (1991) 335.
[32] F. Prokert, H. Ritter, J. Ihringer, Ferroelectrics Lett. 24 (1998) 1.
[33] J. Ravez, A. Simon, C. R. Chimie 5 (2002) 143.
[34] H. El Alaoui-Belghiti, A. Simon, M. Elaatmani, J.-M. Réau, J. Ravez, Phys. Status Solidi 187 (2) (2001) 549.
[35] R. Von Der Mühll, J. Ravez, Bull. Soc. Fr. Mineral. Cristallogr. 98 (1975) 118.
[36] J. Ravez, A. Simon, C. R. Acad. Sci., 3, Ser., Paris, 2000 267.
[37] P.B. Jamieson, S.C. Abrahams, J.L. Bernstein, J. Chem. Phys. 50 (1969) 4352.
[38] E.A. Giess, B.A. Scott, G. Burns, D.F. O'Kane, A. Segmuller, J. Am. Ceram. Soc. 52 (1969) 276.
[39] M.H. Francombe, Acta Crystallogr. 13 (1960) 131.
[40] J. Ravez, B. Elouadi, J.-P. Chaminade, A. Levasseur, P. Hagenmuller, Ferroelectrics 155 (1977) 155.
[41] J. Jerphagnon, J. Phys. Rev. B 2 (1970) 1091.
[42] J. Ravez, A. Perron, P. Hagenmuller, Mater Res. Bull. 10 (1975) 201.
[43] S. Giri, K. Ghoshray, Phys. Rev. B 57 (10) (1998) 5918.
[44] E. Banks, M. Shone, Y.S. Hong, R.F. Williamson, W.O. Boo, Inorg. Chem. 21 (11) (1982) 3894.
[45] Y.S. Hong, R.F. Williamson, K.N. Baker, Y.T. Du, S.N. Seyedahmadian, W.O. Boo, Inorg. Chem. 31 (6) (1992) 1040.
[46] S. Ishihara, J.P. Rivera, E. Kita, Z.G. Ye, F. Kubel, H. Schmid, Ferroelectrics 162 (1–4) (1994) 399.
[47] X.H. Rui, G. Ming, M.X. Lin, Z. Li, W.J. Yang, Jpn J. Appl. Phys. 40 (1) (2001) 202.
[48] J.K. Wang, N. Wakiya, O. Sakurai, K. Shinozaki, N. Mizutani, Key Eng. Mater. 169–170 (1999) 3.
[49] N. Wakiya, J.K. Wang, A. Saiki, K. Shinozaki, N. Mizutani, J. Eur. Ceram. Soc. 19 (6–7) (1999) 1071.
[50] A. Ballman, A. Van Uitert, G. Le Grand, US 3423686 Patent, 1969.
[51] J.-P. Ganne, private communication.